Multiply Scattered Light Tomography and Confocal Imaging: Detecting Neovascularization in Age-related Macular Degeneration

A.E. Elsner[1], M. Miura[1], S.A. Burns[1], E. Beausencourt[1], C. Kunze[1], L.M. Kelley[2], J.P. Walker[1,2], G.L. Wing[1,2] P.A. Raskauskas[1,2], D.C. Fletcher[1,2]

1-Schepens Eye Research Institute, 20 Staniford St., Boston, MA, 02114

2- Retina Consultants of SW Florida, Ft. Myers, FL

Q. Zhou,[3] and A.W. Dreher[3]

Laser Diagnostic Technologies, Inc., San Diego, CA

elsner@vision.eri.harvard.edu

Abstract: A novel technique, Multiply Scattered Light Tomography (MSLT), and confocal Infrared Imaging are used to provide diagnostic information using a comfortable, rapid, and noninvasive method. We investigated these techniques in detecting neovascularization in age-related macular degeneration. The MSLT used a Vertical Cavity Surface Emitting Laser (VCSEL) at 850 nm, while the confocal imaging technique used either the VCSEL or a 790 nm laser diode. Both were implemented into the topographical scanning system (TopSS, Laser Diagnostic Technologies, Inc.) Confocal imaging with both lasers provided different information about neovascularization as a function of focal plane, and different also from MSLT.

OCIS codes: (170.3880 Medical and biological imaging; 330.4300 Noninvasive assessment of the visual system)

freeform keywords: (170.4470) ophthalmology

Introduction

Age-related macular degeneration (AMD), which attacks the photoreceptors in the deepest part of the retina and the retinal pigment epithelial cells beneath them, is the leading cause of blindness in adults in industrialized countries (1). The detection and localization of this type of pathology is frequently based upon outmoded technology never optimized for either AMD or use in older patients. Primary examples include ophthalmoscopy with visible wavelength light that fails to penetrate cataractous lenses, color photography using expensive film, and fluorescein angiography through poor ocular media. The latter is particularly degraded in the case of aging changes, since short wavelength light is used for excitation. We investigated whether confocal imaging with infrared light can detect and localize neovascularization, the most severe complication of AMD, that often leads to severe vision loss.

Before the advent of modern photonics, imaging of human retinal and subretinal tissues was limited by light safety, visible wavelength sources, and low sensitivity detectors. The problems specific to the eye include small pupils, reflections from the surfaces of the cornea and lens, poor ocular media anterior to the retina, poor return of light from the retinal and subretinal layers, long-range scatter over large retinal areas, and uncontrollable eye movements. Technical advances in the past two decades have improved light efficiency, the sampling of light from target tissues, and the speed of image formation.

One major advance is laser scanning, in which a narrowly focused laser beam illuminates different retinal loci sequentially (2-4). An image is formed digitally, so that optical cross-talk between retinal locations is eliminated. There is no long-range scattered light to reduce the contrast of an image, which is a main problem with conventional fundus photography. Another advantage is the enormous reduction of light needed for a good quality image. This increases safety and greatly improves comfort.

A second major advance is the confocal design of imaging instruments, with an accessible focal plane conjugate to the target tissue, in which apertures are inserted (5-6). The light returning from the target, in this case the retina, is controlled by use of an aperture. A pinhole aperture aligned with the optical axis of the instsrument is used to emphasize light that is directly backscattered from retina, and therefore can pass through the narrow aperture. These are called confocal images. However, confocal apertures can include a variety of shapes, not only the circular pinhole with a central free zone, but also a slit, a pinhole that is offset from the optical axis, or an annular aperture with a central stop. The annular apertures, offset pinhole, or offset slit all block light that is directly backscattered from the plane of focus (7-11). The collected light is often of smaller magnitude per unit free zone of the aperture. Scattered light can be either an insignificant or a dominant portion of an image acquired without benefit of confocal apertures. Annular apertures collect mainly light multiply scattered from the plane of focus, or scattered from out of focus planes. Conventional fundus photography lacks apertures; light returning from a large illumination area is collected. Research fundus camera optics with confocal apertures have been used to great advantage, without laser scanning, to measure spectra from retinal locations (11-12).

novel illumination sources

Laser scanning has made possible a much broader range of laser sources (7-11, 14). Of particular interest is near infrared light, with data from human eyes dispelling the misconception that the point spread function is uselessly broad. Once used to provide a retinal reflection of gross features to indicate that the eye was open, infrared images now visualize clinically useful, deeper structures unattainable with other methods (7-11, 12-16). Several new types of solid state lasers had their first imaging or biomedical application in laser scanning ophthalmoscopes, e.g. Ti:SaF, Cr:Li:SaF, and Vertical Cavity Surface Emitting Lasers (VCSELs) (4,11).

types of scanning laser instruments

Scanning laser instrumentation for laboratory use has had a variety of realizations (2-9, 17), but the two main types of scanning laser ophthalmoscopes with commercial markets have significant differences in optical design and intended use. One was developed by Webb and colleagues, initially marketed by Rodenstock Instrumente (Ottobrunn-Riemerling, Germany), to image the eye with the lowest possible amount of light (2-3, 7-11). The image also provides monitoring during functional measurements (18). The light efficiency is accomplished by the use of a small illumination beam in the center of the entrance/exit pupil of the instrument. Light returning from ocular structures is sampled in the remaining annular region, which covers nearly all of the dilated human pupil. The pinhole apertures in this instrument are typically a minimum of 100 μm in the plane of the retina. This fairly large pinhole, combined with the exit pathway not sampling the light returning at the highest angle from the retina, provides an image containing information from a fairly thick section of tissue.

Laser scanning ophthalmoscopes derived from the Heidelberg University group have much smaller confocal pinholes, to sample directly backscattered light. The apertures are similar in size (27-40 μm) to the beam focused on the retina in all three types of instruments (10-30 μm). These instruments are commercially available from Laser Diagnostic Technologies (San Diego, CA) and Heidelberg Engineering (Heidelberg, Germany). Topographical information is derived from a series of images acquired sequentially from varying focal planes. These tomographic instruments have a beam separator/combiner and symmetric entrance/exit pupils of 3 - 3.5 mm diameter. With the beamsplitter, smaller exit pupil, and small pinhole, more light is needed to form an image. Present instruments use near infrared or red sources to avoid excessive absorption by retinal and choroidal tissues.

The optics of the eye impose limitations on the axial transfer function of light returning from the retinal and subretinal layers, the resulting function having more than 10 times the half-width compared with that found in confocal microscopy. To remedy this, correction of the aberrations of the eye often has been suggested, and the first approach was with deformable mirrors in a laser scanning tomographic instrument (19). Processing of grayscale information is another current approach.

interaction of light and tissue

Equally important to improving the optics of the instrumentation is the modelling of light-tissue interactions in the living retina. Geometric structures such as fluid-filled lesions such as retinal cysts or subretinal new vessels have been shown to alter the light-tissue interactions more than mere optical corrections can overcome, providing useful clinical information (8,10,13,15-16, 20-27). Elevated lesions include cysts, edema around macular holes, pigment epithelial detachments, choroidal neovascularization, and macular edema. The vitreo-retinal interface, or nerve fiber layer, often returns far more light than deeper or more superficial layers. The relative axial location of this brightest layer has been used to perform calculations of relative heights across the retina. A single-peaked transfer function has been a typical assumption, although several authors have used the additional peaks, inflections, or width of the function (23-26). As the retina often is elevated over such lesions, the relative height of the brightest structures across the surface indicates the three-dimensional extent of pathology. An exception is when a cyst in the retina contains sufficient fluid, then the highest peak in the axial transfer function is beneath the retinal surface.

All imaging modalities, whether confocal imaging with reflected light, interferometry, or polarimetry depend upon the distribution of index of refraction changes. Tissues that lack a strong index of refraction change within a narrow enough region, situated in a configuration perpendicular to the illumination beam, produce weak direct backscatter, interference fringes, or polarization signals. A decrease in signal can be interpreted as absorption, variations in the geometry of the tissues with respect to the illumination beam, or lack of the necessary index of refraction change to result in backscatter. Multiply scattered light can result from light-tissue interactions following forward scatter, as well as the generally accepted backscatter from out-of focus planes and lateral scatter off tissues that are poor absorbers. Multiply scattered light, like dark field microscopy, can elucidate structures not visualized or amenable to measurements with directly backscattered light.

We have previously used confocal imaging to study exudation in age-related macular degeneration with exudative lesions (13,22,23). These are characterized by the formation of new blood vessels that leak. Typically these originate from beneath the retina, from the choroidal circulation, and are poorly visualized by many techniques employing visible wavelength light. This is particularly true for pathology beneath the macular pigment. Recently, we showed that exudative lesions that are high, particularly with respect to their diameters, are strongly correlated with severe vision loss. We interpret these data as indicating that there are complex or multiple sources of neovascularization and a build-up of fluid, with these cases typically involving not only the choroidal vasculature, but the retinal vasculature as well. This can directly damage the neural elements of the retina.

We use confocal imaging and a new technique, multiply scattered light tomography (MSLT), which utilizes light that is scattered multiple times without being swamped by a strong signal from directly backscattered light in the plane of focus. Our goal was to detect and localize neovascularization in AMD in a rapid, non-invasive method. The height maps from confocal tomography are objective, while the MSLT provides new opportunities to use differing sources of light for computations. We present new data showing that confocal images from different focal planes provide different information, despite the broad axial transfer function of the human eye.

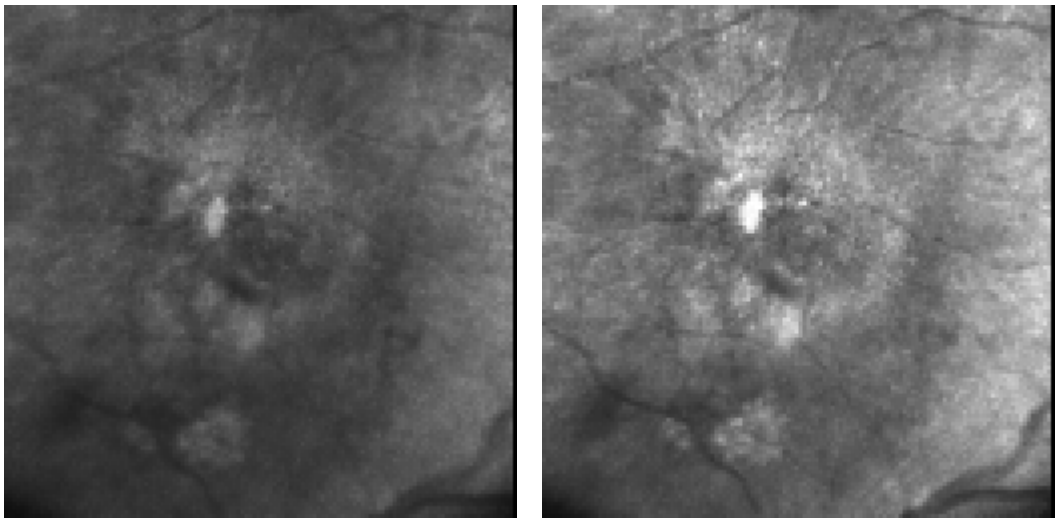

Fig. 1. Left- TopSS individual images at 790 nm, showing the ocular fundus of a 77 yr old female with bilateral exudative AMD. The neovacularization in the four images in this series is visualized by the dark, turbid fluid that elevates the retina, the very dark regions of hemorrhage, and the bright regions of hard exudes that have leaked from the new blood vessels. Left- image 4 from the most anterior section, which is anterior to the retina. Right- image 9, which is slightly deeper, but still anterior to the retina.

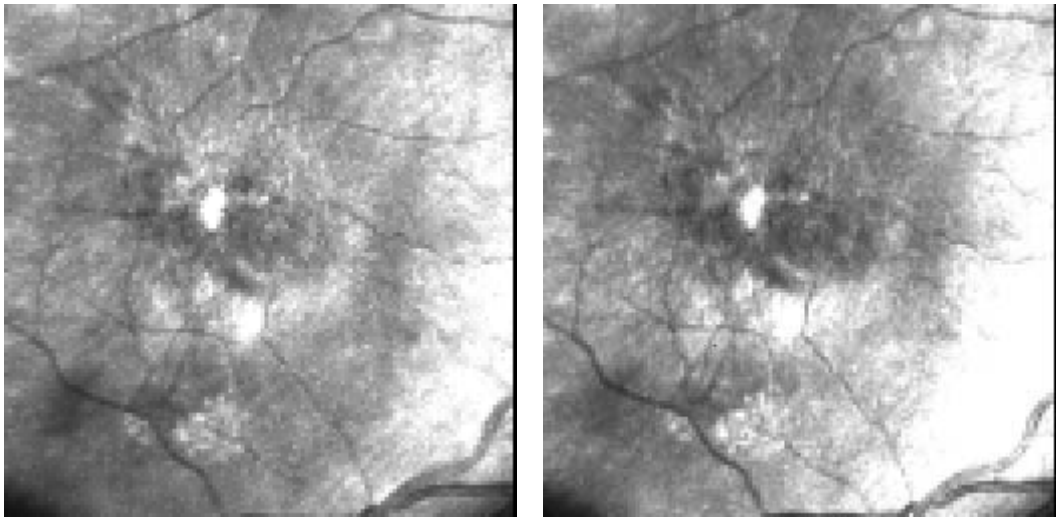

Fig. 2. Left- Same patient as in Fig. 1, but TopSS image 14, which is the in the focal plane of the surface of the retina. Right- TopSS image 19, deep retina: 735μm from the retinal surface. The margin of the RPE tear, inferior to and left of the central portion is clearest in the image of deeper retina.

Methods

Confocal image series were acquired and height measurements were made with a Topographic Scanning System TopSS^{TM} (Laser Diagnostic Technologies, Inc., San Diego, CA). The TopSS^{TM} uses near infrared illumination, penetrating moderate cataract or cloudy media. In a large segment of the aging population, cloudy media or small pupils are present. The illumination is readily tolerated, and the instrument is optimized for a 3 mm pupil. Data acquisition consists of 32 sections acquired from anterior to posterior, sequentially in 0.9 sec. Each 256 x 256 pixel image may be acquired as a 10 x 10, 15 x 15, or 20 x 20 deg field. Two illumination sources were used: a 790 nm laser diode or the center element of an 850 nm VCSEL (VIXEL Corp., Broomfield, CO), aligned on axis with the confocal pinhole (11). Additional optics were introduced so that the VCSEL beam was collimated, and the laser spacing on the retina was minified to 47 μm. The pinhole size was 40 μm in diameter with respect to the

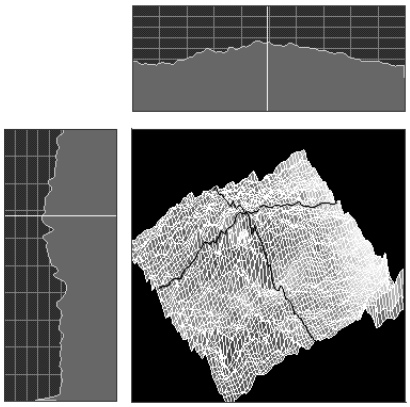

Fig. 3. Wire frame representation of the elevation of the retina over the subretinal new vessels and fluid. Far more reflective than most of tissues in the deeper layers, vitreo-retinal interface or the nerve fiber layer is the origin of the majority of the light returning from the fundus in a confocal image

retina, while the usual TopSS^{TM} pinhole is 24 μm. MSLT image series were acquired simultaneously with the confocal image series, using line-by-line alternation of the center laser with the surrounding 8 lasers that were off-axis with respect to the pinhole.

Individual image sections or averages of 2-4 images produced using a Matlab program (MathWorks, Natick, MA) as well as the calculations from a series of 32 images. To obtain full information for the three-dimensionality of structures, a cross-sectional approach was taken. Intensity values, or the intensity difference values, were plotted to form a height map or a cross-sectional image from the 32 sections in the x,z plane. The Matlab program allows any x,z or y,z plane to be selected by the operator, according to the feature of interest.

Results

Confocal tomography (CT) of a 77 year old female patient with AMD showed exudation (Figs. 1-3). Visual acuity was severely reduced: 20/300 in the right eye and 20/200 in the left. A dilated fundus examination of the right eye showed a serous retinal detachment of the macula. The fluorescein angiogram of the right eye revealed a classic choroidal neovascularization with a retinal pigment epithelial tear, seen in the confocal images. Exudation in an 82 yr old male is shown in Figs. 4-5.

CT and MSLT both visualized features of exudation in AMD. Individual sections provided distinctly different views (Figs. 1-5, link 29). Both confocal imaging and MSLT gave information concerning the lateral extent of the exudative lesions, with the confocal images indicating the elevation and distortion of the retina. Subretinal fluid appears dark with respect to the surrounding retina for both imaging modes. The MSLT images showed the borders of exudative lesions beneath the retina, while minimizing the fairly uniform layers of fluid located anterior to the new vessel membranes. In contrast,

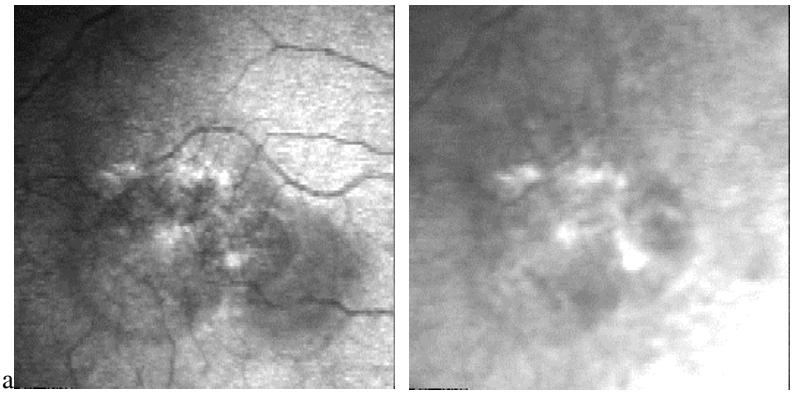

Fig. 4. L:eft- Confocal image series of 32 images from an 82 yr old male patient with exudative AMD from Ft. Myers, FL. There is good light return only for some of the sections in the middle of the series, when the superficial layers are in the plane of focus. Right- Corresponding 32 MSLT images, taken at the same time as the confocal series, with line-by-line alternation.

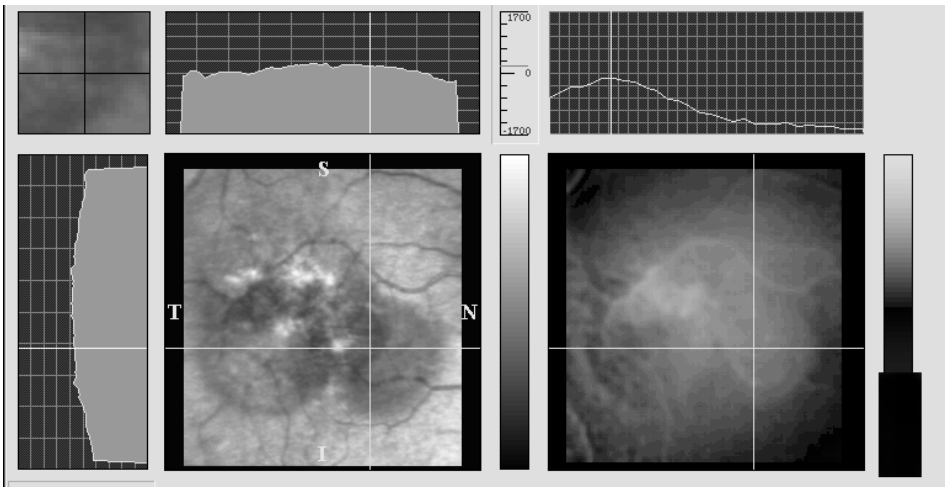

Fig. 5 confocal cross section, showing raised retina over fluid and single band of reflection

CT emphasized the retinal features, including the elevation and deformation of the retinal nerve fiber layer by subretinal exudation. CT emphasizes small exudates beneath the retina. Live MSLT images provide the added cue of focusing and motion parallax, and the lesion is localized in seconds.

Discussion

Confocal tomography and MSLT provided a rapid, noninvasive method to detect and localize macular degeneration and pathological structures found in eyes of older patients. There were clear-cut differences among images from different focal planes. Adequate depth resolution is demonstrated for the evaluation of potential fluid detachment of the neurosensory retina, an important clinical finding.

Acknowledgements: Supported by EY0762 and Wold Foundation to A.E.E., EY12178 to A.W.D., and DE-FG 02-91ER61229 to Dr. Robert H. Webb.

References, notes, and links:

1. H. Leibowitz, D. E. Kruger, L. R. Maunder, R. C. Milton, M. M. Kini, H, A. Kahn, R. J. Mickerson, J. Pool, T. L. Colton, J. P. Ganley, and J. Loewenstein, "The Framingham Eye Study Monograph: an ophthalmological and epidemilogical study of cataract, glaucoma, diabetic retinopathy, macular degeneration, and visual acuity in a general population of 2631 adults, 1973-1975," Surv. Ophthalmol. 24(Suppl) 335-610 (1980).
2. R. H. Webb, GW Hughes, and O. Pomerantzeff, "Flying spot TV ophthalmoscope," Appl. Optics 19 2991-2997 (1980).
3. R. H. Webb and G. W. Hughes, "Scanning laser ophthalmoscope," IEEE Trans. Biomed. Eng. 28 488-492 (1981).
4. W. Dreher and R. N. Weinreb, "Accuracy of topographic measurements in a model eye with the laser tomographic scanner," Invest. Ophthalmol. Vis. Sci. 32 2992-2996 (1991).
5. R. H. Webb, G. W. Hughes, and F. C. Delori, "Confocal scanning laser ophthalmoscope," Appl. Optics, 26 1492-1499, 1987.
6. E. Dreher, P.C. Tso , and R. N. Weinreb, "Reproducibility of topographic measurements of the normal and glaucomatous optic nerve head with the laser tomographic scanner,". Am. J. Ophthalmol. 111 221-229 (1991).
7. A review of the early infrared scanning laser techniques may be found in A. E. Elsner, A. H. Jalkh, A.H, and J. J. Weiter, "New devices in retinal imaging and functional evaluation," in *Practical Atlas of Retinal Disease and Therapy*, W. Freeman, ed. (Raven, New York, 1993) pp. 19-35. The work of several groups is found in

A. E. Elsner, D.-U. Bartsch, J. J. Weiter, and M. E. Hartnett, "New devices in retinal imaging and functional evaluation," in *Practical Atlas of Retinal Disease and Therapy*, W. Freeman, ed. (Lippincott-Raven, New York, 1998) 2nd edition, pp. 19-55.

8. E. Elsner, A.E. Burns, S.A., Kreitz, M.R., and Weiter, J.J. New views of the retina/RPE complex: quantifying sub-retinal pathology, Noninvasive Assessment of the Visual System, Technical Digest, Optical Society of America 1 150-153 (1991).
9. E. Elsner, A.E., Burns, S.A., Hughes, G.W., and Webb, R.H. Reflectometry with a Scanning Laser Ophthalmoscope. Applied Optics 31 3697-3710 (1992).
10. E. Elsner, S. A. Burns, J. J. Weiter, and F. C. Delori, "Infrared imaging of subretinal structures in the human ocular fundus," Vision Res. 36 191-205 (1996).
11. E. Elsner, A. W. Dreher, Q. Zhou Q, E. Beausencourt, S. A. Burns, R. H. Webb, "Multiply scattered light tomography: vertical cavity surface emitting laser array used for imaging subretinal subretinal structures," Lasers and Light in Ophthalmology 8 193-202 (1998).
12. F. C. Delori, "Spectrophotometer for noninvasive measurement of intrinsic fluorescence and reflectance of the ocular fundus," Appl. Optics 33 7439-7452 (1994).
13. L. M. Kelley, J. P. Walker, G. L. Wing, P. A. Raskauskas, and A. E. Elsner, "Scanning laser ophthalmoscope imaging of age related macular degeneration and neoplasms," J. Ophthalmic Photography 3 89-94 (1997).
14. E. Elsner, S. A. Burns, J. J. Weiter, and M. E. Hartnett, "Diagnostic applications of near infrared solid-state lasers in the eye," LEOS '94, IEEE Catalog number 94CH3371-2, Library of Congress number 93-61268, 1, 14-15 (1994).
15. M E. Hartnett and A. E. Elsner, "Characteristics of exudative age-related macular degeneration determined in vivo with confocal direct and indirect infrared imaging," Ophthalmol. 103 58-71 (1996).
16. M. E. Hartnett, J. J. Weiter, G. Staurenghi, and A E. Elsner, "Deep retinal vascular anomalous complexes in advanced age- related macular degeneration," Ophthalmol. 103 2042-2053 (1996).
17. J. F. Le Gargasson, F. Rigaudiere, J. E. Guez, A. Gaudric, and Y. Grall, "Contribution of scanning laser ophthalmoscopy to the functional investigation of subjects with macular holes," Doc. Ophthalmol. 86 227-238 (1994).
18. J.-F. Chen, A. E. Elsner, S. A. Burns, R. M. Hansen, P. L. Lou, K. K. Kwong, and A. B. Fulton, "The effect of eye shape on retinal responses," Clinical Vision Sciences 7 521-530 (1992).
19. W. Dreher, J. F. Bille, and R. N. Weinreb RN, "Active-optical depth resolution improvement of the laser tomographic scanner," Appl. Optics 28 804 (1988).
20. Remky, O. Arend, A. E. Elsner, F. Toonen, M. Reim, and S. Wolf, "Digital imaging of central serous retinopathy using infrared illumination," German J. Ophthalmology 4 203-206 (1995).
21. E. Beausencourt, A. E. Elsner, M. E. Hartnett, and C. L. Trempe, "Quantitative analysis of macular holes with scanning laser tomography," Ophthalmology 104 2018-2029 (1997).
22. Kunze, A. E. Elsner, E. Beausencourt, L.Moraes, M. E. Hartnett, and C. L. Trempe, "Spatial Extent of Pigment Epithelial Detachments in Age-related Macular Degeneration," Ophthalmology 9 1830-1840 (1999).
23. E. Beausencourt, A. Remky, A. E. Elsner, M. E. Hartnett, C. L. Trempe, "Infrared scanning laser tomography of macular cysts," Ophthalmology 107 376-385 (2000).
24. D.-U. Bartsch, M. Intaglietta, J. F. Bille, A. W. Dreher, M. Gharib, W. R. Freeman, "Confocal laser tomographic analysis of the retina in eyes with macular hole formation and other focal macular diseases," Am. J. Ophthalmol. 108 277-87 (1989).
25. D.-U. Bartsch and W. R. Freeman, "Axial intensity distribution analysis of the human retina with a confocal scanning laser tomograph," Exp. Eye Res. 58 161-173 (1994).
26. Hudson F. G. Flanagan, G. S. Turner, D. McLeod, "Scanning laser tomography Z profile signal width as an objective index of macular retinal thickening," Br. J. Ophthalmol. 82 121-30 (1998).
27. Jaakkola, E. Vesti, I. Immonen I, "The use of confocal scanning laser tomography in the evaluation of retinal elevation in age-related macular degeneration," Ophthalmology 106, 274-9, (1999).
28. The link to additional figures is http://color.eri.harvard.edu/annhom.htm.
29. The link to updates on available infrared scanning laser topographic instrumentation is http://www.laserdiagnostic.com.